STRESS ANALYSIS OF BONDED JOINTS IN PULTRUDED GRP COMPONENTS

S.W. Boyd*, J. M. Dulieu-Barton*, O. T. Thomsen, A.Gherardi***
[J.M. Dulieu-Barton]: janice@soton.ac.uk
***University of Southampton, UK **Aalborg University, Denmark**

Keywords: *Bonded joints, pultrusion, thermoelastic stress analysis.*

Abstract

Thermoelastic stress analysis is used to determine the stress field in an orthotropic pultruded material. An economical means of experimentally obtaining the thermoelastic constant and some mechanical properties of each of the constituent materials in the pultruded structure is devised. The stresses in a bonded joint are obtained using thermoelastic stress analysis. The calibrated thermoelastic data is used to validate a finite element model of the joint. It is shown that to accurately interpret thermoelastic data from a layered structure, such as that of the pultrusion, calibration is an essential step. It is also demonstrated that the thermoelastic approach provides an excellent means of validation of finite element models.

1 Introduction

Pultruded composites are manufactured by pulling fibres that have been immersed in resin through a heated die. Alternatively, the resin may be injected into the heated die, thus enabling a completely closed process. The material is layered, usually with the main component being a thick layer of unidirectional material (UD). This is often sandwiched between outer layers of a randomly orientated material. These outer layers give transverse and shear strength to the pultruded material and can be made up of either chopped strand mats (CSM) or combination mats (CM). A combination mat is formed by a chopped strand mat stitched on a woven roving mat, giving a stronger profile; CM is used in the current work. For protection purposes, a thin layer of material, known as a 'surface veil', is usually deposited on the surface. In the current work the surface veil consists of thermoplastic fibres wetted with polyester resin. Pultruded materials have been used in civil engineering structures. A good example of their application is small bridges, such as Wilcott Bridge and West Mill Roadbridge in England. However a lack of confidence in their properties has restricted their use in large structures, although their use is increasing in both Europe and North America. In the marine industry there is a possibility that pultruded materials could be used in superstructures. For this to be adopted, it will be necessary to connect lengths of pultruded material to form a larger structure. Bolted connections have been studied, e.g. [1, 2]. However the major drawback here is the stress concentration at the hole that may act as a damage initiator; furthermore bolts add mass. Investigations into bonded pultruded *butt strap* joints have been carried out, e.g. [3], where it was shown that the joint efficiency was poor. This was attributed to damage initiating in the UD/CSM material interface, as a result of poor interlaminar mechanical properties.

To identify a means of increasing the joint efficiency it is necessary to establish the stress distribution in the joint and the surrounding pultruded material. This will define how the load is carried and transferred to each layer. To do this an experimental technique known as thermoelastic stress analysis (TSA) [4] is used to obtain quantitative stress data. TSA is a non-contact technique that provides a full field stress map of a component. The TSA will provide a new insight into pultruded joint behaviour, to enable improvement of the joint design and validation of Finite Element Analysis (FEA).

2 Pultruded material characterisation

The pultruded composite material used for this study was a 140 x 10 mm strip profile of polyester resin and E-glass reinforcement. The profile was

supplied by Fiberline Composites A/S in Denmark. Within the pultruded profile a number of E-glass reinforcement types were used: UD rovings that make up the majority of the reinforcement content and a CM containing a layer of woven roving stitched to a layer of CSM.

The aim of the material characterisation is to determine the material properties of each of the constituent materials in the pultrusion. Fig. 1 shows a micrograph of the pultruded material and clearly shows the various materials present; i.e. the outer CM, the resin rich areas and the central UD core. Of particular importance here is the resin rich pockets trapped between the UD core and the fabric layers of CM that lead to the reduced interlaminar strength.

In Fig. 1 there are essentially three 'layers' in the pultruded material: the central unidirectional rovings and the outer CM. Although these layers are not uniform throughout the pultrusion, to obtain dimensions of each layer the average thickness of each layer was determined from micrographs measurements. The average dimensions of the layers contained in the nominally 10 mm thick profile are 2.22 and 2.48 mm for the upper and lower CM respectively and 5.12 mm for the UD. There was a 7% variation in the measurements.

Tensile test specimens with dimensions of 250 x 25 x 10 mm were cut from the pultruded strip profile. These specimens were subjected to a tensile load using a 50 kN electro-mechanical Instron test machine and a 50 mm gauge length extensometer. The average Young's modulus was determined as 29.4 GPa with a coefficient of variation of 3.8%. The fibre volume fraction of 46% was determined by a burn off test.

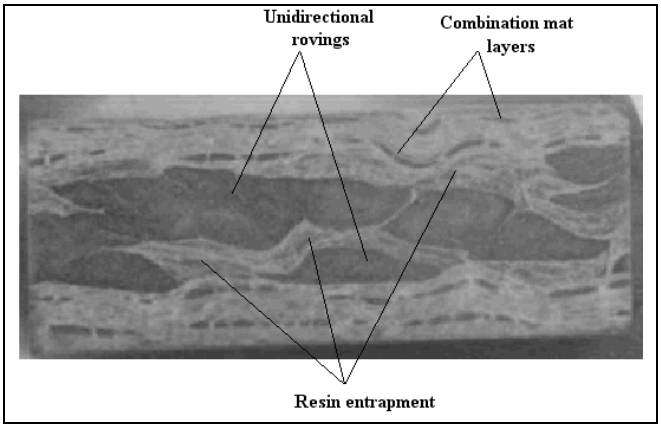

Fig. 1. Micrograph of pultruded section

To accurately model the entire pultrusion, the elastic properties of each constituent within the pultrusion must be obtained. It was not practical to obtain pultrusions of each of the constituent layers due to the prohibitive costs associated with the manufacture of the dies for such small production runs. Therefore to obtain specimens representative of each of the pultrusion constituent layers it was decided to simulate the pultrusion process using the application of heat and pressure in an autoclave to produce a vacuum consolidated laminate. Samples of the individual reinforcements and samples of the pultrusion resin were provided by Fiberline. The fibre volume fraction was chosen as the metric to determine if the *pseudo-pultrusion* was representative of the actual pultrusion. Full details of the process and its validation are given Ref. [5].

Panels of the UD material, CM and the resin were manufactured using the *pseudo-pultrusion* process so that specimens from each could be used to determine Young's modulus. The density of the material was determined experimentally, and burn-off tests were conducted to determine the fibre volume fraction. Tensile specimens were cut from each panel and tested in an electro-mechanical Instron test machine using a 50 kN load cell and a 50 mm gauge length extensometer. The results are presented in Table 1 and show a relatively high unidirectional laminate material stiffness. The values in Table 1 are consistent with the values obtained for the entire pultruded section; the Young's modulus and volume fraction for the UD are greater and for the CM are less.

Table 1 Constituent material properties

Layer	***Young's Modulus (CoV)***	***Fibre Vol Fraction (CoV)***
UD	35.0 GPa (4.1%)	0.55 (1.4%)
CM	13.2 GPa (5.2%)	0.39 (3.1%)
Resin	2486 MPa (12%)	-

3 Thermoelastic stress analysis: background

TSA is a well-established technique that has been used in a wide range of engineering applications, e.g. [4]. TSA uses a highly sensitive infra-red detector to measure the temperature changes induced in a material as a result of the thermoelastic effect. The temperature change (ΔT) is directly related to the stress change. The working equation for orthotropic materials, such as that obtained from pultrusion, is:

$$\Delta T = -\frac{T}{\rho C_p}\left(\alpha_{11}\sigma_{11} + \alpha_{22}\sigma_{22}\right) \quad (1)$$

where T is the absolute temperature of the specimen surface, ρ is the density, C_p is the specific heat at constant pressure, α_{11} and α_{22} are the coefficients of thermal expansion in the principal material directions and σ_{11} and σ_{22} are the direct stresses in the principal material directions.

In the present research a Cedip Silver infrared thermography system is used to determine ΔT. It is possible to rewrite equation 1 as follows:

$$\Delta T = K_1 T \Delta\sigma_{11} + K_2 T \Delta\sigma_{22} \quad (2)$$

where $K_1 = \alpha_{11} / \rho C_p$ and $K_2 = \alpha_{22} / \rho C_p$.

Rearranging equation 2 provides an expression in terms of stress rather than temperature change as follows:

$$\frac{\Delta T}{K_1 T} = \Delta\sigma_{11} + \frac{K_2}{K_1}\Delta\sigma_{22} \quad (3)$$

4 Thermoelastic stress analysis: calibration

The thermoelastic constant K_1 of each of the constituent materials can be determined experimentally from a uniaxial tensile test. In a simple tensile test the second term on the right hand side of equation 3 is eliminated as $\Delta\sigma_{22} = 0$ so that the calibration constant, $A^* = \Delta T/\Delta\sigma_{11}=K_1 T$, for each material can be obtained. This is then used to calibrate ΔT in to stress terms as follows:

$$\frac{\Delta T}{A^*} = \Delta\sigma_{11} + \frac{K_2}{K_1}\Delta\sigma_{22} \quad (4)$$

This means the TSA data is calibrated to give a stress metric and provides data in the form of a full field ‘stress’ map. It is unnecessary to obtain K_2 to calibrate the thermoelastic data. However, it is necessary to obtain K_2 to make comparisons or validate finite element data, i.e. the FE must be presented in the form of the right hand side of equations 3 and 4.

To obtain K_1 for the UD and CM layers, specimens were prepared using the pseudo-pultrusion method discussed in section 2. Knowing the cross sectional area of the specimens and applying a known tensile (uniaxial) load, the stress in the specimen can be determined. The major assumption here is that $\Delta\sigma_{22}$ is eliminated from equation 4 by the uniaxial loading (see above). In the UD specimen this is valid. In the through-thickness plane of the CM this was also considered valid, as the transverse fibres would not provide any traction that results in a finite transverse stress. A validation of these assumptions is provided in Ref. [4]. ΔT was obtained for each specimen type subjected to a cyclic tensile stress ($\Delta\sigma_{11}$), and therefore the calibration constants for both the unidirectional and combination layers in the longitudinal direction were obtained as 874 MPa°K^{-1} and 384 MPa°K^{-1} respectively. Experimentally obtaining the transverse calibration constants has been set aside as the type of specimen necessary to obtain this would be difficult to manufacture and therefore it was decided to use approximations of K_2 in the FEA to assess the influence of this quantity.

5 Thermoelastic stress analysis of adhesive joints

To construct the joint, coupons were cut from the 10 mm thick pultruded plank using a table mounted water cooled diamond impregnated circular saw. Two adherend coupons with nominal dimensions of 150 x 50 x 10 mm and two strap coupons with dimensions of 100 x 50 x 10 mm made up each double butt strap joint, as shown schematically in Fig. 2. The components of the joints were bonded using a two-part epoxy adhesive Araldite 2015. A light abrasion surface preparation was conducted followed by a solvent wipe prior to bonding. The joints were allowed to cure at room temperature for 24 hours and were post cured at 50°C for a further 24 hours. A photograph of the joint is shown in Fig. 3. In the photograph the cut surface of the pultruded section can be seen, and the inhomogeneous nature of the material is apparent even at this scale. The bond line is apparent and of relatively uniform thickness of approximately 0.5 mm. The spew fillets are not even on each side of the joint. In general the joint is representative of the type of joint that would be constructed in practice, i.e. not perfectly uniform or symmetrical.

For the thermoelastic stress analysis calibration K_1 for the pultruded layers in the longitudinal direction were obtained experimentally as described above. For the adhesive the thermoelastic constant was obtained using values from the literature providing a thermoelastic constant (K) for the adhesive of 2.88 x 10^{-5} MPa^{-1}. Using the known test temperature (300 K), the calibration constant for the adhesive of 115.7 MPa°K^{-1} was obtained.

The double lap joint specimen was subjected to a mean load of 8 kN with a cyclic load amplitude of 5 kN. Fig. 4a shows the thermoelastic signal from the upper half of the strap joint. This increases the resolution of the TSA data and allows detailed data to be obtained from the spew fillet and end of the strap. Fig. 4b provides the calibrated stress data. In Fig. 4b there appears to be little stress in the adhesive. However, there is a stress concentration present within the strap on the left hand side of the joint at the location equivalent to the interface between the CM and the UD layers. In addition, there is a stress concentration at the spew fillet. In the main adherend there appears to be an increase in stress in the region of the strap ends. Again this is concentrated at the interface between the unidirectional and combination layers. Fig. 4b therefore demonstrates clearly that the differences in the mechanical properties of the materials contained in the pultruded joint are the cause of stress concentrations within the pultruded material and ultimately may lead to the interlaminar failure of the joint.

It has been shown that the layers of material in the pultrusion have different mechanical properties, and therefore the thermoelastic constants and the stress field within an adhesively bonded pultruded joint are dictated by the layered nature of the pultrusion. Thus, it would be inefficient to examine every joint or pultrusion using experimental techniques such as thermoelastic stress analysis. Therefore, the following sections of the paper concentrate on the production and validation of an FE modelling approach for the design of adhesive joints in pultruded material.

6 FE model

The joint was modelled using the ANSYS FEA package using 2-D, 8-noded quadrilateral elements (PLANE82). In order to reduce the error in the loading of the model, the whole joint was modelled, and the load was applied away from the bonded region. Initially a coarse model was produced. It was assumed that a pressure load applied to the ends of the model reproduced the stress field induced by the test machine grips in the experimental work. The boundary conditions for the coarse model were therefore such that the upper adherend was fully constrained, and the pressure load was applied to the lower adherend to generate a tensile stress. The adherends and adhesives were assumed to be perfectly connected as the previous work [3] showed that the failure of the joints occurs within the adherend material.

Some of the mechanical properties of each layer of the pultrusion were calculated from the experimental tests conducted in Section 2. The remainder were obtained either from literature or through calculation. The adopted material properties are detailed in Table 2. The joint was divided into areas of specific materials, i.e. the unidirectional core, the combination outer layers and the adhesive. The latter is defined as an isotropic material with material properties obtained form the manufacturer. The pultrusion layers were defined with anisotropic material properties. All materials were assumed linear elastic as the load applied during the testing produced less than 40% of the ultimate strength of the pultrusion.

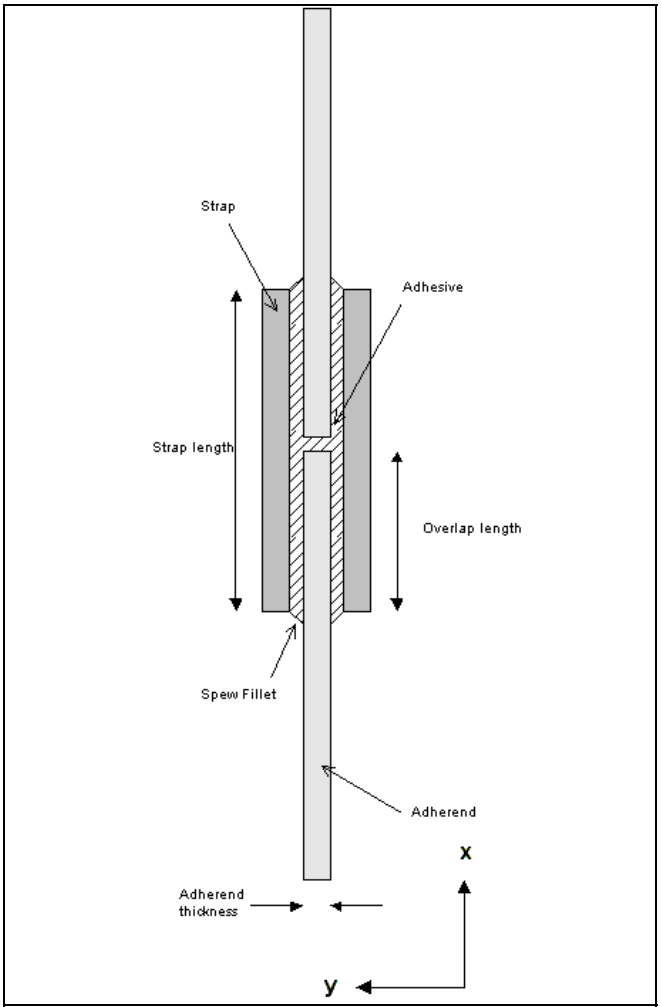

Fig. 2. Schematic of a double butt strap joint

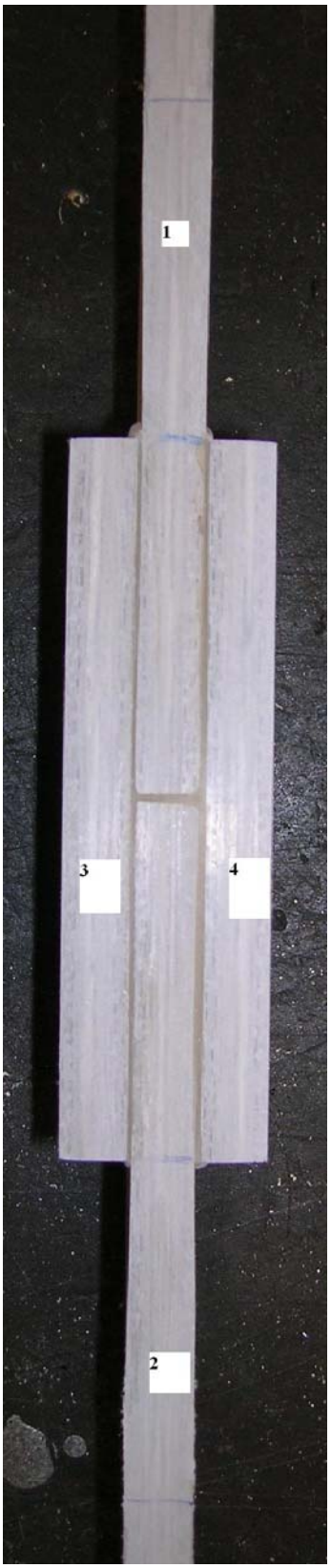

Fig.3. Photograph of butt strap joint

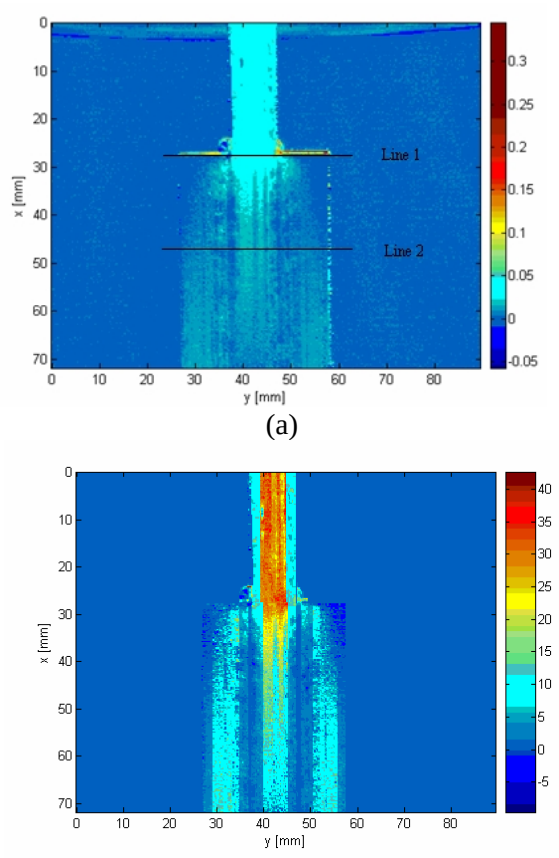

(a)

(b)

Fig. 4. Thermoelastic signal (a) and calibrated stress (b) plot of upper portion of double strap joint

Table 2 Material properties for the FEA

Material	E_x *(MPa)*	E_y*(MPa)*	v_{xy}	G_{xy}*(MPa)*
Unidirectional	35575 [a]	3500 [b]	0.28 [d]	1367 [e]
Combination	15542 [a]	3500 [b]	0.28 [d]	1367 [e]
Adhesive	2000 [c]	2000 [c]	0.36 [c]	735 [e]

[a] Property obtained from experiments in Section 2
[b] Property obtained from Ref. [6]
[c] Property obtained from manufacturers data sheet
[d] Property obtained from Ref. [7] for 55% fibre volume fraction glass/epoxy
[e] Property from calculation

Sub modelling was employed so that a much finer mesh was constructed allowing a detailed examination of features. This allowed the introduction of the spew fillets, which were modelled as triangular sections with the triangular side being twice as long as the thickness of the adhesive as was used as the equivalent spew fillet by Frostig et al. [8]. The upper portion of the double

butt strap, equivalent to that examined experimentally as shown in Fig. 4, was modelled by the sub model. The boundary conditions for the sub model were interpolated from the coarse model by imparting displacement boundary conditions on the sub model. The boundary stresses for both the coarse and sub models were compared to ensure continuity between the two models. The mesh used for the sub model is shown in Fig. 5a. The mesh density is such that the adhesive layer and the inner combination mat appear as the solid black areas in the figure. In fact the adhesive layer is half the width of the spew fillet.

To directly compare the FEA results to the calibrated TSA results it is necessary to obtain the quantity K_2 as an input for the FEA (see equation 4). It was decided to use values for the resin (α, ρ and C_p) obtained from the manufacturer, giving a value of 4.8 x 10^{-5} MPa^{-1}, as an upper bound, and to assume $K_2 = K_1$ as the lower bound in the FEA. Figure 5b shows the FE results for the lower bound data.

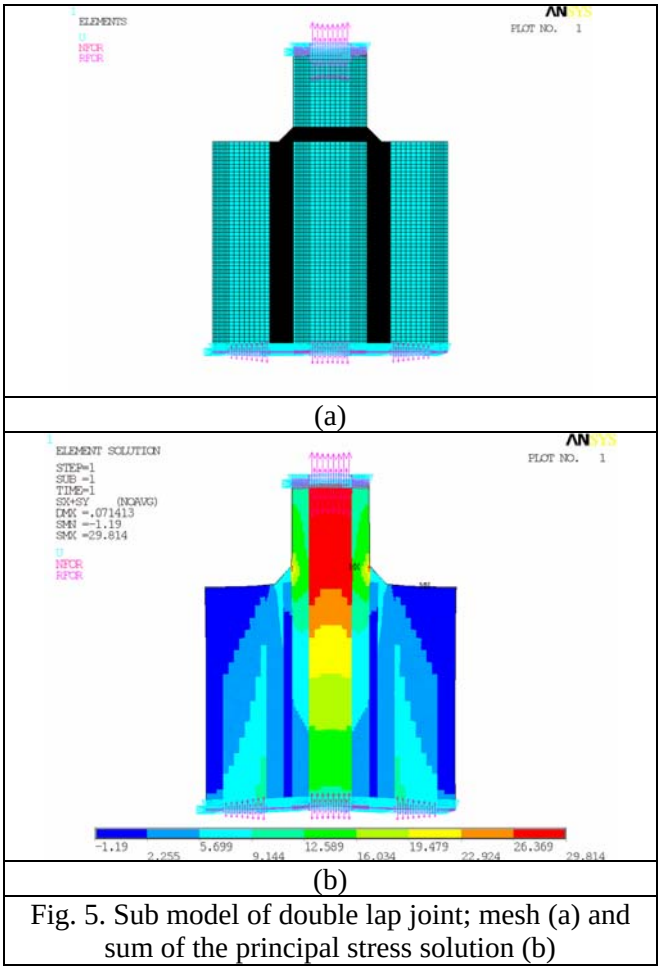

Fig. 5. Sub model of double lap joint; mesh (a) and sum of the principal stress solution (b)

7 Discussion

Line data was obtained from the TSA across the adhesive joint at 2 locations (see Fig. 4a); at the end of the butt strap overlap, and 20 mm from the end of the butt strap overlap. The principal stresses were obtained from the FE analysis in the same locations, manipulated according to equation 4 and the results are presented in Fig. 6 for the upper and lower bounds of K_2. Figure 6a shows the results at the end of the strap overlap, and an excellent correlation between the numerical and experimentally derived results is observed, particularly for the transitions between the different layers of the pultrusion.

In Figure 6a the upper and lower bound numerical results straddle the experimental results suggesting that the K_2 parameter is not equal to K_1, nor is it equal to the value obtained for pure resin, but somewhere in between. This implies that there is some interaction between the resin and fibres in the through thickness direction. The interaction is particularly relevant in the combination mat of the central adherend where the FEA is greatly over predicting the stress. A lower value of K_2 in this area (due to some through thickness matrix fibre interaction) will reduce the numerical model prediction. The same is true of the unidirectional core with the lower bound K_2 corresponding well in some areas, which are probably resin dominated, and the upper bound over predicting as K_2 for the material is likely to be less than that for the resin. Clearly a means for experimentally evaluating K_2 is required to improve the accuracy of the FE results. Therefore the correlation between the numerical and experimental results in Figure 6a could only be defined as moderate. However, an inspection of Figure 6b shows a much better correspondence in all areas of the joint, apart from the adhesive. Here only the lower bound FE results are shown as $\Delta\sigma_{22}$ in this region will be close to zero. This is because the material properties from the adhesive were taken from the literature; and a better correlation would be expected if the K value for the adhesive could be obtained experimentally.

Overall, the correlation between the numerical and experimental results is good. However, in some areas of Figures 6a and b the experimental are very noisy and differing greatly from the relatively smooth numerical results. This can be attributed to the inhomogeneous nature of the pultruded material. The micrograph provided in Figure 1 shows that there are areas in the unidirectional core that contain a large amount of resin.

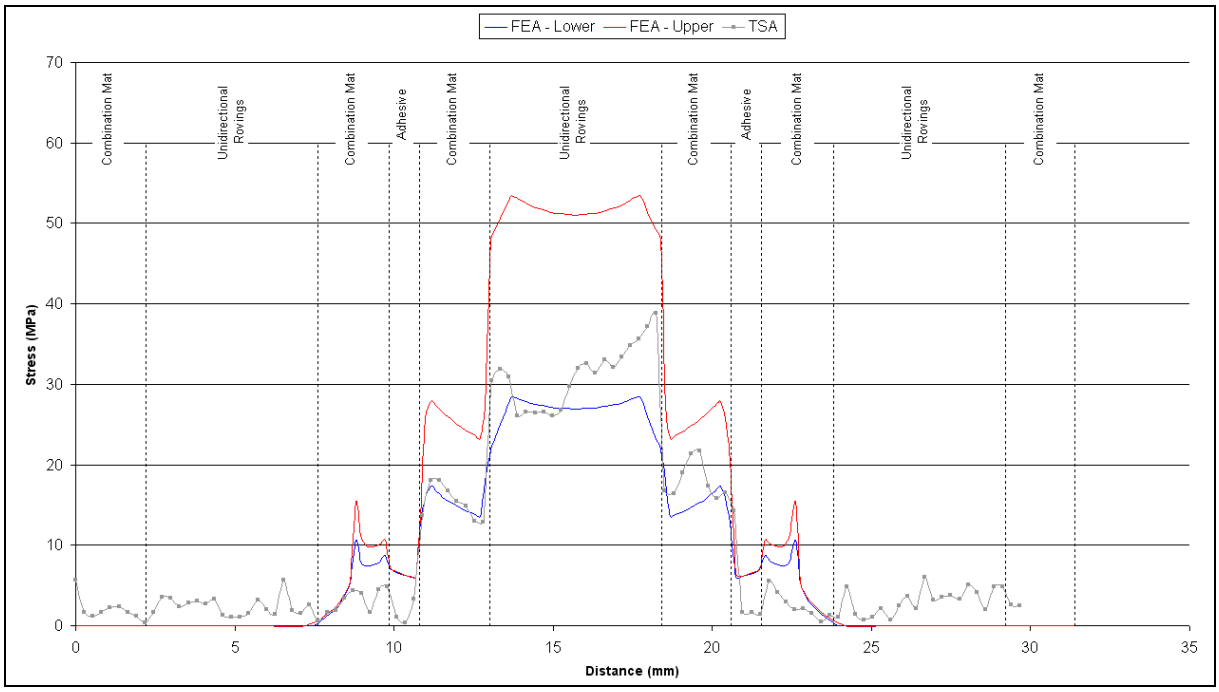

(a)

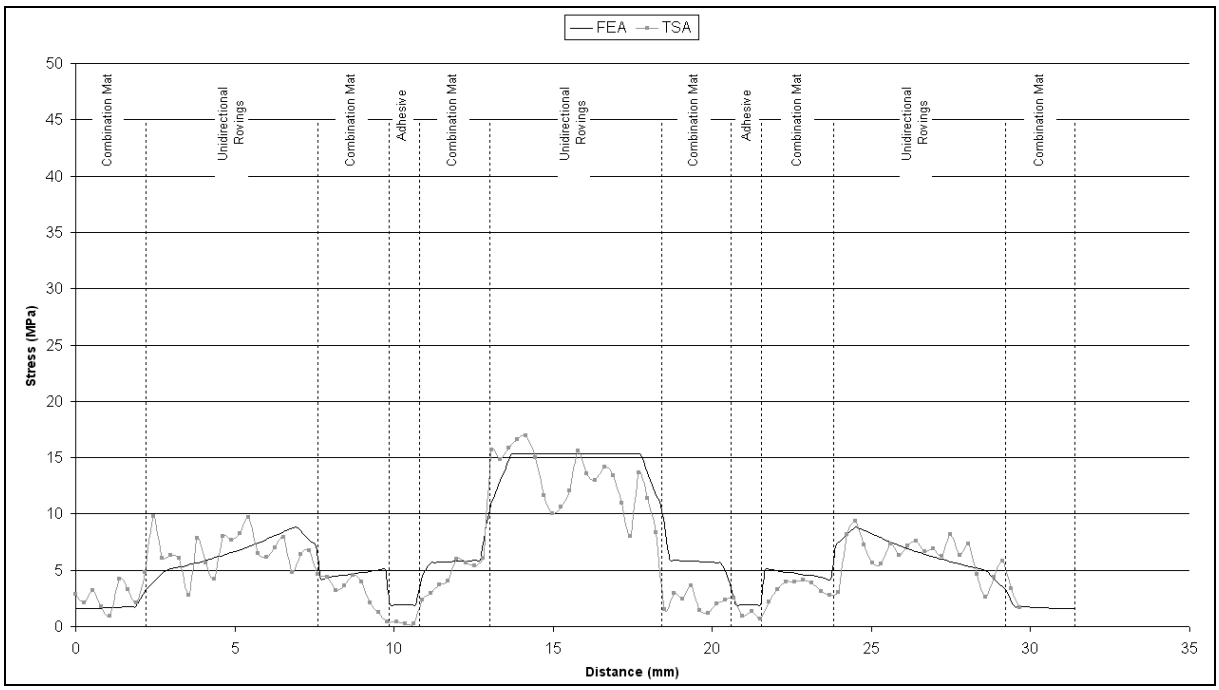

(b)

Fig. 6. comparison of numerical and experimental plots of stress from Lines 1 (a) and 2 (b) shown in Figure 4 (a)

These areas have not been included in the numerical model because of the random nature of the resin entrapment. Likewise the experimental TSA signals from the resin rich areas, again due to their random locations, were not calibrated using the calibration constant for the resin material. This will result in an incorrect calculation of the stress in these localised regions, and hence the variable nature of the experimental curve presented in Figures 6a and b. However, in general the numerical and experimental results correlate well in the interface

areas of the joint, e.g. in the transition from the combination layers to the epoxy adhesive.

The overall correspondence between the FE and the TSA provides confidence in the numerical modelling technique, as it has been validated using experimentally derived data. In addition, it further confirms the validity of the material property data obtained from the pseudo-pultruded material to represent the actual pultruded lay-up. The even better correlation between the experimental and numerical results is obtained away from the end of the overlap (Figure 6b). In addition, the non-ideal geometry of the experimental specimens resulting in stress concentration levels experimentally not observed in the idealised numerical model.

8 Conclusions

The work in this paper has shown:

1. It is possible to create a pseudo-pultrusion material using a combination of vacuum consolidation, elevated temperature and increased pressure in an autoclave to create test materials for the calibration of the thermoelastic data and for obtaining material properties as input to a finite element model.
2. The thermoelastic signal was calibrated using the experimentally derived calibration constants for each of the constituent materials in the pultrusion. This allowed the examination of experimental data for stress concentrations in the through thickness direction during loading of double lap joints in pultruded material
3. A FE model was created using the material properties obtained from the pseudo-pultrusion and validated with the experimental data from the TSA. The correlation between the two data sets was very good. This gives confidence in the modelling approach and allows for further examination of the bonded joint numerically to further understand the failure mechanisms and examine possible ways of improving the performance of adhesively bonded joints in pultruded material.
4. Further work is required to experimentally obtain the K_2 value for the pultruded material constituent materials, in particular in the combination mat, in order to improve the numerical modelling prediction.

Acknowledgements

The authors are grateful to Fiberline Composites A/S (Middelfart, Denmark) for the supply of pultruded materials and the dry reinforcements and liquid resins for the pseudo-pultruded manufacture.

References

[1] Bank, L. C., Mosallam, A. S., and McCoy, G. T., "Design and performance of connections for pultruded frame structures." *Journal of Reinforced Plastics and Composites*, 13, 1994, pp 199-212

[2] Turvey, G. J. and Cooper, C., "Review of tests on bolted joints between pultruded GRP profiles." *Proc.of the Institution of Civil Engineers Structures and Buildings*, 157, 2004, pp 211-233

[3] Boyd, S. W., Winkle, I. E., and Day, A. H., "Bonded butt joints in pultruded GRP panels - an experimental study." *International Journal of Adhesion and Adhesives*, 24(3), 2004, pp 263-275

[4] Dulieu-Barton, J. M. and Stanley, P., "Development and applications of thermoelastic stress analysis." *Journal of Strain Analysis*, 33, 1998, pp 93-104

[5] Boyd, S. W., Dulieu-Barton, J. M., Thomsen, O. T., and Gherardi, A., "Development of a finite element model for analysis of pultruded structures using thermoelastic data." Submitted April 2007.

[6] Keller, T. and Vallee, T., "Adhesively bonded lap joints from pultruded GFRP profiles. Part II: joint strength prediction." *Composites Part B*, B36, 2005, pp 341-350

[7] Daniel, I. and O. Ishai, *Engineering Mechanics of Composite Materials.*Oxford University Press, 1994.

[8] Frostig Y., Thomsen, O. T., and Mortensen, F, "Analysis of adhesive-bonded joints, square-end, and Spew-Fillet-high-order theory approach." *Journal of Engineering Mechanics*, 125(11), 1999, pp 1298-1307